

Efficient Visible-Light Photocatalytic Water Splitting by Minute Amounts of Gold Supported on Nanoparticulate CeO₂ Obtained by a Biopolymer Templating Method

Ana Primo,[†] Tiziana Marino,^{†,‡} Avelino Corma,[†] Raffaele Molinari,[‡] and Hermenegildo García^{*,†}

[†]Instituto de Tecnología Química (CSIC-UPV), Universidad Politécnica de Valencia, Av. de los Naranjos s/n, 46022 Valencia, Spain.

[‡]Department of Chemical and Materials Engineering, University of Calabria, Via P. Bucci, 44/A, I-87036 Rende, CS, Italy

S Supporting Information

ABSTRACT: When irradiated with visible light ($\lambda > 400$ nm) 1 wt % gold-supported ceria nanoparticles generate oxygen from water ($10.5 \mu\text{mol}\cdot\text{h}^{-1}$) more efficiently than the standard WO₃ ($1.7 \mu\text{mol}\cdot\text{h}^{-1}$) even under UV irradiation ($9.5 \mu\text{mol}\cdot\text{h}^{-1}$). This remarkable photocatalytic activity arises from a novel preparation method to reduce the particle size of ceria (5 nm) by means of electrostatic binding of Ce⁴⁺ to alginate gel, subsequent supercritical CO₂ drying, and calcination. The low loading of Au is crucial for the observed high catalytic activity.

There is an urgent need for developing efficient photocatalytic systems for water splitting since they eventually can lead to the production of solar fuels.^{1–4} In spite of the large research effort in the field of photocatalysis for visible-light water splitting, the number of semiconductors that have decent photocatalytic activity under visible-light illumination is still limited, and the vast majority of the studies are carried out with modified TiO₂.^{4–6} In the overall water splitting, water becomes reduced to hydrogen and simultaneously oxidized to oxygen. Of these two semi-reactions, hydrogen generation is considered simpler since, in principle, the process consists in protons present in the water accepting electrons and noble metals acting as hydrogen evolution centers. In contrast to the simplicity of hydrogen generation, formation of oxygen from water is conceptually more challenging since mechanistically it has to occur through several steps requiring four positive holes and the formation of O–O bonds.^{7,8} For this reason, oxygen evolution is frequently the bottleneck determining the overall efficiency in the overall photocatalytic water splitting. Both semi-reactions, hydrogen and oxygen generation from water, can be independently studied by adding during the photocatalytic process sacrificial electron donors (for hydrogen generation) and electron acceptors (for oxygen formation). Therefore, it is possible to decouple both semi-reactions and focus the study on one of them. Considering the importance in developing novel efficient photocatalysts with visible-light activity with comparable or higher efficiency than those currently known^{9–11} and also the interest in having efficient semiconductors for oxygen evolution, in the present contribution we describe that nanoparticulated ceria prepared by a novel biopolymer-templating methodology and containing appropriate gold loadings is a stable and efficient photocatalyst for oxygen evolution. The relevance of our finding is

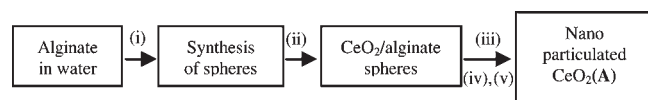
two-fold. On one hand, our report shows how, by reducing the particle size down to the nanometer scale, a conventional metal oxide insulator is converted into a semiconductor whose photocatalytic activity strongly depends on the particle size in the nanometer scale. On the other hand, we show that by supporting gold nanoparticles it is possible to introduce visible-light response in the nanoparticulated ceria that otherwise would be inactive under visible-light irradiation. Part of our work is based on a novel preparation method of very small nanoparticle-sized ceria using a biopolymer (alginate) as template with the resulting nanoparticulated ceria exhibiting a high photoactivity as a semiconductor. It is well documented that conventional ceria of large particle size behaves as insulator devoid of any photocatalytic activity.^{12,13} Scattered precedents have reported that reducing the particle size of ceria to the nanometer scale introduces some photovoltaic activity.¹⁴ In general most of the interest in nanoparticulated ceria derives from the field of heterogeneous catalysis wherein the role of ceria is just as catalyst support.^{15,16} Characterization of nanoparticulated ceria shows that, by reducing the size to the nanoscale, two general effects occur, namely the creation of framework oxygen defects and confusion of Ce +3/+4 oxidation states. The semiconductor activity observed here derives probably from these two types of structural defects appearing when nanoparticles are prepared. The most active sample for the visible-light photocatalytic generation of oxygen reported here (CeO₂(A)) was prepared as indicated in Scheme 1.

The first step consists in the anionic exchange Ce⁴⁺ into alginate dissolved in water that precipitates when a sufficient large uptake of Ce⁴⁺ is achieved. At this point the Ce⁴⁺ loading determined by chemical analysis was 77.5 wt %. The subsequent step in the synthesis is the supercritical CO₂ drying of the sample that requires a prior gradual exchange of water for ethanol since, in contrast to ethanol, water is immiscible in supercritical CO₂. The supercritical CO₂ drying is crucial, as has already been demonstrated,^{17,18} to achieve a highly porous alginate with remarkably high surface area. In our case, at this moment Ce⁴⁺ ion is still compensating for the negative charge of carboxylate groups present in the biopolymer. Figure 1 shows an image of the millimetric alginate spheres obtained by coagulation of the aqueous alginate solution with Ce⁴⁺ as well as a representative TEM image of the corresponding material. Isothermal N₂ adsorption measurements give a specific surface area for alginate

Received: February 15, 2011

Published: April 20, 2011

Scheme 1. Biopolymer Templated Synthesis of CeO₂(A) Nanoparticles^a



^a i) Alginate precipitation by (NH₄)₂Ce(NO₃)₆; ii) maturation (19 h); iii) water by ethanol exchange; iv) supercritical CO₂ drying; v) air calcination.

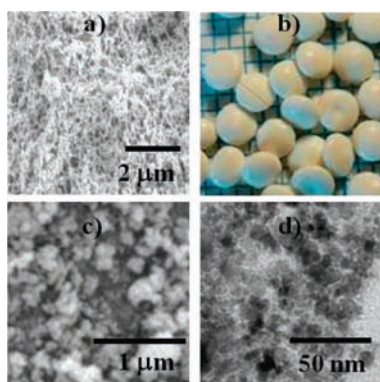


Figure 1. (a) SEM of uncalcined CeO₂(A); (b) uncalcined spheres; (c) SEM of calcined CeO₂(A); (d) TEM Au(1.0 wt %)/CeO₂(A).

containing Ce⁴⁺ of 229 m² × g⁻¹. This sample was submitted to mild aerobic calcination to effect the controlled combustion of the biopolymer and formation of CeO₂(A). The novel CeO₂(A) material was characterized by conventional techniques in material sciences. Thus, XRD shows that CeO₂(A) is crystallized in the fluorite phase (see Supporting Information [SI] Figure S1) and also XPS shows that most of the Ce atoms (over 90%) are in the +4 oxidation state (see SI Figure S2). BET surface area measurement gives a value of 93 m² × g⁻¹. The average particle size of CeO₂(A), determined by counting a statistical relevant number of nanoparticles, was 4.9 ± 0.1 nm. Overall, the data obtained are consistent with a well-crystallized CeO₂(A) sample with a 5 nm particle size and a large specific surface area that originates from the templating effect of alginate dried under supercritical CO₂.

For the sake of comparison with CeO₂(A) we have included in our study also a commercial nanoparticulate CeO₂ sample (CeO₂(B) from Aldrich). XRD and BET measurements (see SI Figure S3) indicate that CeO₂(B) has the same crystal phase as CeO₂(A), similar surface area (102 m² × g⁻¹) and larger average particle size (20 nm) than CeO₂(A) sample. Also in our study we have used WO₃ as a reference photocatalyst for oxygen generation.⁸ It is generally considered that WO₃ is a benchmark material for oxygen generation to which novel photocatalysts should be compared to establish relative efficiencies. The SI contains relevant data for the WO₃ material employed in the present work. Besides the ceria photocatalyst, our study also includes the visible-light photocatalytic activity of ceria-supported gold nanoparticles (Au/CeO₂(A) and Au/CeO₂(B)). Au/CeO₂ are important heterogeneous catalysts for low-temperature CO oxidation, alcohol oxidation, and aromatic amine carbamoylation among other reactions.¹⁹ Due to its ample use in heterogeneous catalysts, there is a considerable amount of information about the Au/CeO₂ preparation. The most widely

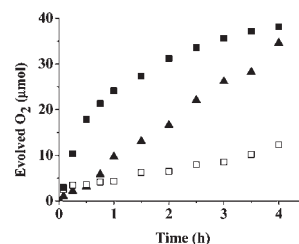


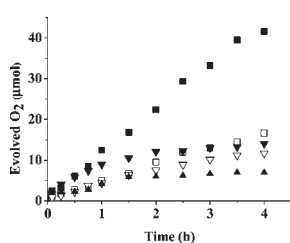
Figure 2. O₂ evolution upon UV irradiation of an aqueous suspension of AgNO₃ containing: ■ WO₃, ▲ CeO₂(A), and □ CeO₂(B).

used procedure is the so-called deposition–precipitation method.¹⁹ Here we have followed this procedure and deposited gold nanoparticles on CeO₂(A) at two different loading levels (see SI). In the literature there is much current interest in determining whether the presence of noble metal nanoparticles increases or decreases the photocatalytic activity of a semiconductor.²⁰ In particular in the case of titania there are contradictory reports describing negative and positive influences on titania photocatalytic activity by the presence of gold nanoparticles.²⁰ Recently, we have shown that, while under UV illumination the photocatalytic activity of titania decreases because gold acts under these conditions as electron/hole recombination center, under visible-light irradiation the situation drastically changes, and then the presence of gold is beneficial because it introduces visible-light photoactivity by irradiation at the surface plasmon band of gold.²¹ Considering the controversial influence of noble metals on semiconductor photoactivity it is of current interest to determine here how the photoactivity of ceria is influenced by gold, as well as to determine the influence of loading on the efficiency. In the present work we carried out photocatalytic experiments for oxygen generation from water under UV and visible irradiation. The data presented below show that the influence of gold favoring or disfavoring the photocatalytic activity is different, depending on the UV or visible irradiation wavelength. Photocatalysis under visible-light irradiation is considerably more challenging due to the lower photon energy that is generally unable to excite wide band gap semiconductors and also because about 45% of the solar light corresponds to the visible range. However, herein the initial experiments with ceria materials were performed with UV light with the aim of obtaining data supporting the photocatalytic activity of this metal oxide for oxygen generation from water. Experiments submitting a suspension of CeO₂ or Au/CeO₂ in water containing EDTA or methanol as sacrificial electron donors failed to generate hydrogen in the range of pH 1–7. In contrast analogous experiments using Ag⁺ or Ce⁴⁺ as electron scavengers gave rise to the photocatalytic generation of oxygen. In accordance with earlier precedents,⁸ we also observed that Ag⁺ promotes oxygen evolution with higher efficiency than when Ce⁴⁺ was used. Figure 2 shows the temporal profile of oxygen evolution under UV irradiation of CeO₂(A) and CeO₂(B). For the sake of comparison we also include the photocatalytic behavior of WO₃ as reference. As can be seen in Figure 2, although WO₃ exhibits a high initial rate under these conditions as well as a slightly higher oxygen amount generated by the end of the reaction, the relevance of the obtained data is that both ceria materials exhibit photocatalytic activity for oxygen generation under UV light irradiation.

The temporal profiles for O₂ generation determined for CeO₂(A) and CeO₂(B) are remarkably different. While commercial CeO₂(B) seems to exhibit a higher initial rate, even comparable to that of WO₃, the slope of the O₂ formation curve

Table 1. Photocatalytic Activity (Initial Reaction Rate, r_0 , and Evolved Oxygen at 4 h) of the Series of Materials under Study

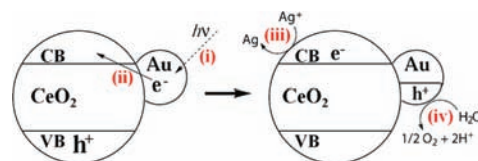
catalyst	UV		vis	
	r_0 ($\mu\text{mol min}^{-1}$)	evolved $\text{O}_{2,4\text{ h}}$ (μmol)	$r_0 \times 10^2$ ($\mu\text{mol min}^{-1}$)	evolved $\text{O}_{2,4\text{ h}}$ (μmol)
CeO ₂ (A)	0.145	34.6	—	—
CeO ₂ (B)	0.07	12.31	—	—
WO ₃	0.452	38.1	6.6	6.9
Au(1.0 wt %)/CeO ₂ (A)	0.104	34.0	20.2	42.0
Au(1.0 wt %)/CeO ₂ (B)	0.075	16.4	9.2	16.7
Au(3.0 wt %)/CeO ₂ (A)	0.051	11.2	18.4	14.1
Au(3.0 wt %)/CeO ₂ (B)	0.037	8.1	8.1	11.8

**Figure 3.** Oxygen evolved upon visible light ($\lambda > 400$ nm) illumination of an aqueous AgNO₃ suspension containing the photocatalyst. ■ Au(1.0 wt %)/CeO₂(A); □ Au(1.0 wt %)/CeO₂(B); ▼ Au(3.0 wt %)/CeO₂(A); ▽ Au(3.0 wt %)/CeO₂(B); ▲ WO₃.

decreases remarkably even at short times. In contrast in the case of CeO₂(A) the initial reaction rate was smaller, but it maintains the activity over the time and after 45 min is more efficient than CeO₂(B), reaching photocatalytic activity comparable to that of WO₃ at 4 h. These differences can be rationalized, considering that CeO₂(B) undergoes fast deactivation, probably by deposition of Ag particles, under these conditions. In contrast, CeO₂(A) with the smaller particle size becomes more active due to its lower tendency to deactivate. When ceria samples containing gold nanoparticles at 1.0 or 3.0 wt % were tested under the same conditions, it was observed that the presence of gold at 3 wt % loading is highly detrimental for the photocatalytic efficiency. However, with regard to the final moles of oxygen formed, samples with 1.0 wt % Au loading exhibit photocatalytic activity similar to that of ceria without gold. Table 1 summarizes the initial reaction rates and final moles of oxygen formed for the photocatalysts studied.

It can be concluded that under UV irradiation the presence of Au plays a minor (1.0 wt %) or notable (3.0 wt %) negative influence on the photocatalytic activity of CeO₂ under UV irradiation.

On the basis of precedents using TiO₂ as a photocatalyst containing noble metal nanoparticles,²⁰ we propose that the negative influence of gold is due to the role of Au nanoparticles acting as charge (e^-/h^+) recombination centers when the semiconductor is excited in the band gap. Photocatalytic experiments using UV light similar to those previously referenced were performed under visible light ($\lambda > 400$ nm). Under these conditions CeO₂(A) or CeO₂(B) did not give rise to the generation of any oxygen. Only WO₃ exhibited a low photocatalytic oxygen generation activity in agreement with its low performance under

Scheme 2. Elementary Steps Occurring in the Photocatalytic Oxygen Evolution upon Irradiation of Au/CeO₂ with Visible Irradiation^a

^ai) Photon absorption; ii) electron injection from Au to ceria conduction band; iii) electron quenching by Ag⁺; iv) water oxidation by h⁺.

visible light illumination. In sharp contrast, all the Au/CeO₂ samples exhibited visible light activity. Moreover the photocatalytic activity of Au (1 wt %)/CeO₂(A) using visible light was higher than that achieved with CeO₂(A) under UV irradiation. This behavior is remarkable because, typically for titania and other semiconductors, the photocatalytic activity under UV is considerably reduced using visible light, whereas here the performance for Au/CeO₂ can be better using visible light. It is remarkable that with the use of Au/CeO₂(A) the final moles of oxygen evolved are higher than those obtained for WO₃ using UV light. Figure 3 shows selected plots of the oxygen formed over the time for visible light illumination for the series of Au/CeO₂. For comparison, we have included also in this Figure 3 the activity of WO₃ under the same conditions. With respect to the influence of Au loading we observed again that 1.0 wt % Au renders a more efficient photocatalyst than 3.0 wt % Au. Also as commented using UV irradiation, the ceria sample prepared by the novel biopolymer template procedure described previously and having smaller particle size is far more efficient than larger particle size in the conversion of commercial CeO₂(B). Concerning the mechanism of O₂ formation, the photo action spectrum of Au/CeO₂(A) was studied using monochromatic light in the range 410–650 nm; the ability to generate O₂ was found to follow the surface plasmon band profile (see SI). This supports that gold nanoparticles are the species responsible for light absorption and trigger the photochemical events. In addition, preliminary experiments using cyclic voltammetry reveal for Au/CeO₂(A) the presence of an oxidation peak at about +1.49 V that is absent in CeO₂. If this were the oxidation potential of the positive holes in Au/CeO₂(A) they would have enough energy to promote water oxidation. In addition, flash photolysis of Au/CeO₂(A) using a 532 nm laser has allowed the detection of transients decaying in microsecond time scale that are compatible with electron injection from photoexcited Au nanoparticles to the conduction band of ceria (see SI). Scheme 2 summarizes our proposal to rationalize the photocatalytic behavior of Au/CeO₂ under visible irradiation.

In summary, herein we have reported the unprecedented photocatalytic activity of ceria nanoparticles for oxygen generation from water. The photocatalytic activity depends on the ceria particle size, and a novel ceria preparation based on templation by alginate is reported. In addition, we have also shown that deposition of gold nanoparticles at low loading increases the photocatalytic activity for visible-light-producing samples that exhibit higher photocatalytic activity than the same material upon irradiation at its bandgap. Moreover, the ceria samples containing gold under visible light irradiation outperform the photocatalytic activity of WO₃ under UV irradiation. Our finding opens the way for using ceria as a photocatalyst for other reactions.

■ ASSOCIATED CONTENT

S Supporting Information. XRD and XPS of CeO₂(A); XRD of CeO₂(B); TEM of Au/CeO₂(B); UV–vis spectra of the samples, characteristics of WO₃; synthesis of nanoparticulated CeO₂(A); deposition–precipitation preparation of Au/CeO₂; photocatalytic tests; photoresponse spectrum of Au/CeO₂(A) for O₂ generation; electrochemical characterization of Au/CeO₂-(A and B); and transient spectra of Au/CeO₂(B). This material is available free of charge via the Internet at <http://pubs.acs.org>.

■ AUTHOR INFORMATION

Corresponding Author

hgarcia@qim.upv.es

■ REFERENCES

- (1) Gust, D.; Moore, T. A.; Moore, A. L. *Acc. Chem. Res.* **2009**, *42*, 1890–1898.
- (2) Kudo, A.; Miseki, Y. *Chem. Soc. Rev.* **2009**, *38*, 253–278.
- (3) Kamat, P. V. *J. Phys. Chem. C* **2007**, *111*, 2834.
- (4) Yerga, R. M. N.; Galvan, M. C. A.; del Valle, F.; de la Mano, J. A. V.; Fierro, J. L. G. *ChemSusChem* **2009**, *2*, 471–485.
- (5) Zhu, J. F.; Zach, M. *Cur. Opin. Colloid Interface Sci.* **2009**, *14*, 260–269.
- (6) Hernandez-Alonso, M. D.; Fresno, F.; Suarez, S.; Coronado, J. M. *Energy Environ. Sci.* **2009**, *2*, 1231–1257.
- (7) Nakamura, R.; Okamura, T.; Ohashi, N.; Imanishi, A.; Nakato, Y. *J. Am. Chem. Soc.* **2005**, *127*, 12975–12983.
- (8) Silva, C. G.; Bouizi, Y.; Fornes, V.; Garcia, H. *J. Am. Chem. Soc.* **2009**, *131*, 13833–13839.
- (9) Maeda, K.; Domen, K. *J. Phys. Chem. C* **2007**, *111*, 7851–7861.
- (10) Maeda, K.; Takata, T.; Hara, M.; Saito, N.; Inoue, Y.; Kobayashi, H.; Domen, K. *J. Am. Chem. Soc.* **2005**, *127*, 8286–8287.
- (11) Zou, Z. G.; Ye, J. H.; Sayama, K.; Arakawa, H. *Nature* **2001**, *414*, 625–627.
- (12) Da Silva, J. L. F.; Ganduglia-Pirovano, M. V.; Sauer, J.; Bayer, V.; Kresse, G. *Phys. Rev. B* **2007**, *75*.
- (13) Lin, C. Y.; Lee, D. Y.; Wang, S. Y.; Lin, C. C.; Tseng, T. Y. *Surf. Coat. Technol.* **2008**, *203*, 480–483.
- (14) Corma, A.; Atienzar, P.; Garcia, H.; Chane-Ching, J. Y. *Nat. Mater.* **2004**, *3*, 394–397.
- (15) Gandhi, H. S.; Graham, G. W.; McCabe, R. W. *J. Catal.* **2003**, *216*, 433–442.
- (16) Gorte, R. J.; Vohs, J. M. *J. Catal.* **2003**, *216*, 477–486.
- (17) Chtchigrovsky, M.; Primo, A.; Gonzalez, P.; Molvinger, K.; Robitzer, M.; Quignard, F.; Taran, F. *Angew. Chem., Int. Ed.* **2009**, *48*, 5916–5920.
- (18) Primo, A.; Quignard, F. *Chem. Commun.* **2010**, *46*, 5593–5595.
- (19) Corma, A.; Garcia, H. *Chem. Soc. Rev.* **2008**, *37*, 2096–2126.
- (20) Primo, A.; Corma, A.; Garcia, H. *Phys. Chem. Chem. Phys.* **2011**, *13*, 886–910.
- (21) Gomes Silva, C.; Juarez, R.; Marino, T.; Molinari, R.; Garcia, H. *J. Am. Chem. Soc.* **2011**, *133*, 595–602.